

CHAPTER 2: PRINCIPLES OF CLOUD AND PRECIPITATION FORMATION

Lead Authors: **William R. Cotton and Sandra Yuter**

In this chapter we provide an overview of the basic physical processes responsible for the formation of clouds and precipitation. A number of important concepts are discussed and terms defined which will be used in later chapters. For more detail on these topics the reader is referred to textbooks by *Pruppacher and Klett* [1997], *Rogers and Yau* [1989], relevant chapters in *Wallace and Hobbs* [2006], *Cotton and Anthes* [1989], and *Houze* [1993] and review articles by *Stewart* [1985] and *Cantrell and Heymsfield* [2005].

2.1 Formation and Structure of Clouds

Different cloud types are defined according to the phases of water present and the temperature of cloud top [AMS Glossary]. If all portions of a cloud have temperatures greater than 0°C it is referred to as a *warm cloud*, or a *liquid phase cloud*. In clouds extending above the 0°C level, precipitation may form either by ice phase or droplet coalescence processes. *Ice-crystal clouds* consist entirely of ice crystals. Analogously, a *water cloud* is composed entirely of liquid water drops. A *mixed-phase* cloud contains both water drops (supercooled at temperatures below 0°C) and ice crystals, without regard to their actual spatial distributions (coexisting or not) within the cloud. Most convective clouds extending into air colder than about -10°C are mixed clouds, though the proportion of ice crystals to water drops may be small until the cloud builds to levels of still lower temperature. Provided the temperature is not below about -40°C, supercooled droplets may coexist with ice particles. However, the liquid phase within unactivated aerosols (haze particles) may coexist with ice particles to very low temperatures.

2.1.1 Dynamical Aspects of Cloud Formation

Clouds form when the saturation vapor pressure becomes smaller than the actual partial pressure of the water vapor in the air. The difference is condensed in the form of liquid water or ice, depending on the temperature. The saturation vapor pressure decreases when the temperature decreases (Clausius-Clapeyron). The most common way clouds form is

therefore when a buoyant parcel of air is lifted (convective ascent) and cooled by adiabatic expansion. For an ascending parcel inside a cloud, the temperature decreases following a moist adiabatic lapse rate which is slightly less (0.65 C per 100 m) than in clear air adiabatic ascent (1 C per 100 m), because of the latent heat released by condensation. The corresponding rate of condensation depends on the temperature and pressure of the cloud cell. For example at 900 m and 20 °C, it is on the order of 2 g/kg per km of ascent. When the cloud base temperature and pressure are determined, the mixing ratio of condensed water at any level above cloud base can be derived as the difference between the water vapor mixing ratio at cloud base and the saturation water vapor mixing ratio at that level. This is referred to as the adiabatic water-mixing ratio. The actual condensed water-mixing ratio is generally lower than the adiabatic value. At cloud base, the condensation of the available water vapor is not instantaneous and the actual water vapor partial pressure can be momentarily higher than the saturation vapor pressure leading to supersaturation. Supersaturation plays a critical role near cloud base for the activation of CCN and IN that initiate cloud droplets (Sec. 2.1.2.1) or ice crystals (Sec. 2.1.2.2). Further, up in the cloud, when cloud particles are numerous and big enough, the rate of condensation keeps pace with the production of supersaturation, so that supersaturations remain steady or decline. The actual condensed water content in a convective cloud is generally lower than the adiabatic one, because the ascending air from the cloud base is continuously mixed with drier air entrained from outside the cloud. The condensed water content, either liquid or ice, is a key parameter for precipitation formation. Precipitation is most likely to form in the regions of largest condensed mixing ratio, i.e. in the least diluted cloud cells.

A second critical parameter is the Lagrangian time scale of the cloud particles, which is the time it takes a parcel of air containing an ensemble of cloud particles to form when entering a cloud, and evaporate or sublimate when the parcel reaches cloud top. Liquid phase precipitation is produced when the numerous but very small droplets, which have grown by condensation, collide and coalesce into a few much larger raindrops with a significant fall speed. Small ice phase particles can grow to precipitation size by any combination of vapor deposition, collection of small water droplets (riming) or collection of other ice particles (aggregation). These processes require significant time, sometimes comparable to or exceeding the lifetime of a cloud. If the Lagrangian time scale of the cloud particles is

shorter than the time needed to produce precipitation, all the condensed water vapor may evaporate in the atmosphere without any precipitation reaching the surface.

The principal types of ascent, each of which produces distinctive cloud forms, are:

Local ascent of warm, buoyant air parcels in a conditionally unstable environment, which produces convective clouds. Because of the release of latent heat, a cloud convective parcel becomes warmer, hence positively buoyant, with respect to its environment. Air parcels within convective cells are thus able to rise into the atmosphere, until they reach a stable boundary such as a temperature inversion or lose their buoyancy by mixing. Convective clouds have diameters from about 0.1 to 10 km and air ascends in them with velocities up to a few meters per second, although updraft speeds of several tens of meters per second can occur within small volumes of large convective clouds. Within stronger updrafts, ascents of a few kilometers typically produce condensed water mixing ratios of a few grams per kilogram. Mixing ratios of more than 10 g/kg are possible in very strong updrafts within deep cumulonimbus clouds.

The lifetimes of convective clouds range from minutes to several hours. The particles Lagrangian time scale though may be shorter. For example, in a shallow cumulus cloud with a depth of ~ 1.5 km and characteristic updraft speeds of 3 m s^{-1} , the Lagrangian time scale is $t_p = 1500 \text{ m} / 3 \text{ m s}^{-1} = 500 \text{ s} \simeq 8 \text{ min}$. This represents the time available for initiation of precipitable particles. Once initiated, precipitation may continue over the remaining lifetime of the cloud. In a towering cumulus cloud with depth of ~ 10 km and updraft speeds of $\sim 15 \text{ m s}^{-1}$, the Lagrangian time scale is $t_p = 10,000 \text{ m} / 15 \text{ m s}^{-1} \simeq 660 \text{ sec} \simeq 11 \text{ mins}$, only slightly longer than shallow cumulus clouds. The main advantage that a towering cumulus cloud experiences over that of a shallow cloud in forming precipitation particles is associated with the greater amounts of condensate that is produced in deeper clouds. Because precipitation growth by collection is a non-linear function of the amount of condensate in a cloud [Kessler, 1969; Manton and Cotton, 1977], precipitation growth proceeds quite rapidly in cumulonimbus clouds relative to low liquid water content cumulus clouds. Supercell storms (~ 12 km depth) have lifetimes of several hours but their strong updrafts ($\sim 40 \text{ m s}^{-1}$), yield a Lagrangian time scale of only $t_p = 12,000 \text{ m} / 40 \text{ m s}^{-1} = 300 \text{ s} = 5 \text{ mins}$, which is shorter than that for shallow cumulus clouds. A characteristic

feature of supercell storms is the bounded weak echo region where updrafts are so strong that there is not sufficient time to produce radar-detectable precipitation elements at mid levels of the storm [*Browning and Ludlam, 1962; Marwitz, 1972*]

Forced lifting of stable air to produce layer or stratiform clouds. Such clouds can occur at altitudes from ground level to the tropopause and extend over hundreds of thousands of square kilometers. Lifting rates range from a few centimeters per second to $\sim 10 \text{ cm s}^{-1}$. Layer clouds generally exist over periods of tens of hours and their Lagrangian time scales are $\sim 10^4 \text{ s}$ ($\sim 3 \text{ hrs}$). Due to their long Lagrangian time scales, precipitation is likely in these clouds in spite of their small water contents ($\sim 0.5 \text{ g kg}^{-1}$).

Forced lifting of air as it passes over hills or mountains to produce orographic clouds. Updraft velocities depend upon the speed and direction of the wind and the height of the barrier, and they can be several meters per second. Water contents are typically a few tenths of a gram per cubic meter of air, depending upon the altitude at which the air enters the cloud upwind and its maximum altitude above the mountain top. Orographic clouds may be quite transitory, but if winds are steady they may last for many hours. However, the relevant time scale that determines the time available for precipitation formation is not the time that it takes a parcel to ascend from cloud base to cloud top. Instead, it is the time that it takes a parcel to transect from the upwind lateral boundary to its downwind boundary, as shown in Figure 2-1. For example, for a 15 m s^{-1} wind speed and a cloud of 18,000 m lateral extent, $t_p = 18,000 \text{ m} / 15 \text{ m s}^{-1} = 1200 \text{ s} = 20 \text{ min}$. This time scale is longer than that for cumulus clouds but considerably shorter than that for layer clouds. Since the liquid water contents of stable, wintertime orographic clouds are low, production of precipitation requires efficient conversion of cloud droplets to precipitation. These conditions can occur in shallow maritime clouds passing over mountains near shore. Lagrangian time scales are longer for deeper mixed and ice-phase orographic clouds as compared to shallower liquid phase clouds. Note that the adiabatic liquid water content for orographic clouds is not determined by the ascent of a cloud parcel from cloud base to cloud top. Instead, it is determined by the vertical displacement of a parcel of air as it transects the cloud over the mountain barrier.

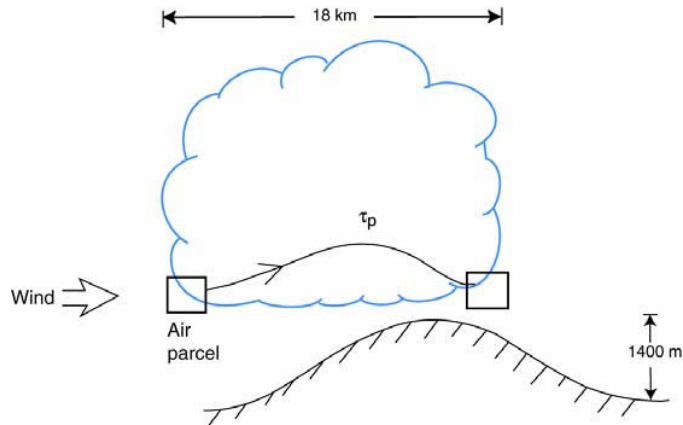


Figure 2-1. Schematic of a stable orographic cloud indicating the trajectory of an air parcel through the cloud, which determines the Lagrangian time scale (t_p) for the development of precipitable particles.

Vertical ascent is not the only way of lowering the temperature and the water vapor saturation pressure. *Cloud top radiative cooling* can lead to destabilization of cloudy layers. This is the main driving force for marine stratocumulus clouds. It is also important in fogs, stratus clouds and cirrus clouds. Longwave radiative flux divergence at cloud top creates cooling of the air, which, in turn, produces higher density air parcels that descend through the cloud layer causing vertical mixing. In the case of a marine stratocumulus layer in which the sea surface temperatures are slightly warmer than the overlying air, the descending cool air parcels can descend through most of the unstable sub-cloud layer, which enhances vertical mixing through the depth of the cloudy boundary layer. Typical lifetimes of stratus and stratocumulus clouds are ~ 6 to 12 h. The Lagrangian time scale for 1000 m deep clouds having vertical velocities of $\sim 0.1 \text{ m s}^{-1}$ is $t_p = 1000 \text{ m} / 0.1 \text{ m s}^{-1} = 10^4 \text{ s} \simeq 3 \text{ h}$. Thus, in spite of the fact that they have liquid water contents of only $\sim 0.1 \text{ g kg}^{-1}$, the long Lagrangian time scales permit the formation of precipitation, in the form of drizzle, in stratus and stratocumulus clouds. Because of cloud top radiative cooling, the temperature at the top of a convective cloud may decrease more than expected from the adiabatic lapse rate, hence leading to a superadiabatic water mixing ratios.

As noted earlier, the above concepts of a cloud are based on simple “back-of-the-envelope” calculations. In general, clouds are very turbulent and thus the time-scales for precipitation

formation can be much longer than simple Lagrangian parcel estimates. Likewise, the liquid water contents of clouds can be quite variable. In cumulus clouds, it is not uncommon to find regions of high liquid water content, say 0.5 to 1.0 gram per cubic meter next to regions with hardly any condensate only tens of meters away. Often cumulus clouds exhibit considerable asymmetry in structure with upshear parts of the cloud experiencing little mixing and turbulence and downshear portions experiencing very large mixing and turbulence. In such a cloud, hydrometeors undergo growth on the upshear side and experience evaporation and turbulence on the downshear.

Thus far, we have only talked about individual cumulus clouds and the lifetimes of individual cells. But in fact, precipitating clouds can affect neighboring clouds by exciting gravity waves, by latent heating induced buoyancy bores and by producing air chilled by evaporation of precipitation particles in the subcloud layer. As illustrated in Figure 2-2 even small cumuli that produce precipitation that evaporates in the sub-cloud layer can form a cold pool. The chilled air is denser than surrounding air and spreads out beneath

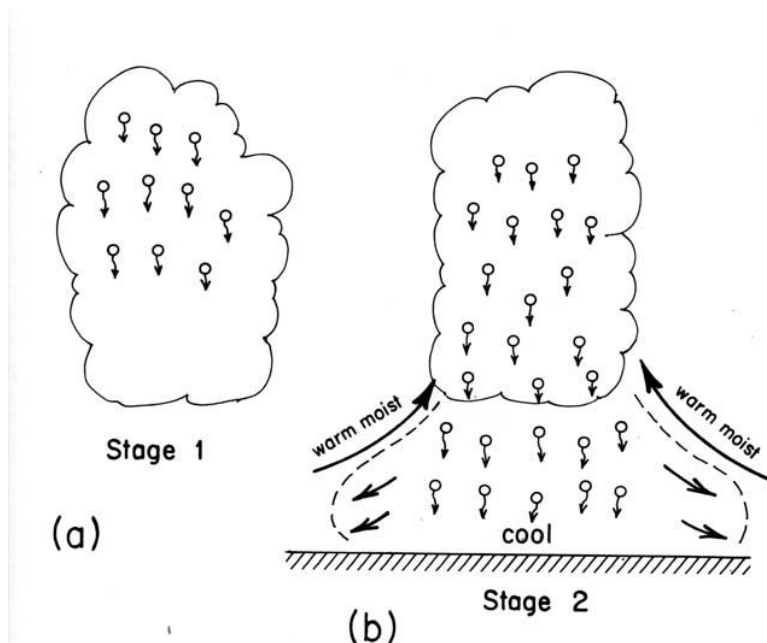


Figure 2-2. (a) Illustration of droplets settling from the upper levels of a cloud, thus reducing the amount of liquid water content or water-loading burden on the cloud. (b) Illustration of the formation of an evaporatively-chilled layer near the surface, which can lift surrounding moist air sometimes to the LCL and LFC. (From Cotton [1990]).

the cloud where it can lift the surrounding air sometimes enough to generate new cloud cells. In some cases neighboring precipitating clouds can produce cool outflows that run into each other and cause lifting of the air leading to the merger of the neighboring clouds (see Figure 2-3). The merged cloud cell is often wider and deeper than the parent clouds and is more likely to produce rain. As illustrated in Figure 2-4 the cold pool and leading edge gust front are important to the maintenance of an ordinary thunderstorm as an efficient engine. The fact that precipitating clouds alter their local environment is important for understanding how pollutants can influence clouds (Chapter 7) and how seeding clouds can perhaps alter precipitation on time scales greatly exceeding the lifetime of individual clouds (Chapter. 8).

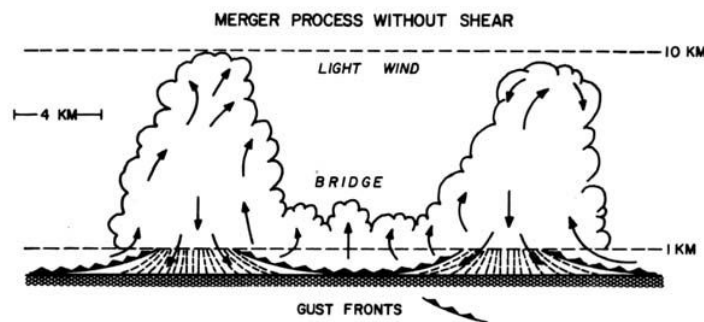


Figure 2-3. Schematic illustration relating downdraft interaction to bridging and merger in case of light wind and weak shear. (From Simpson et al, [1980]).

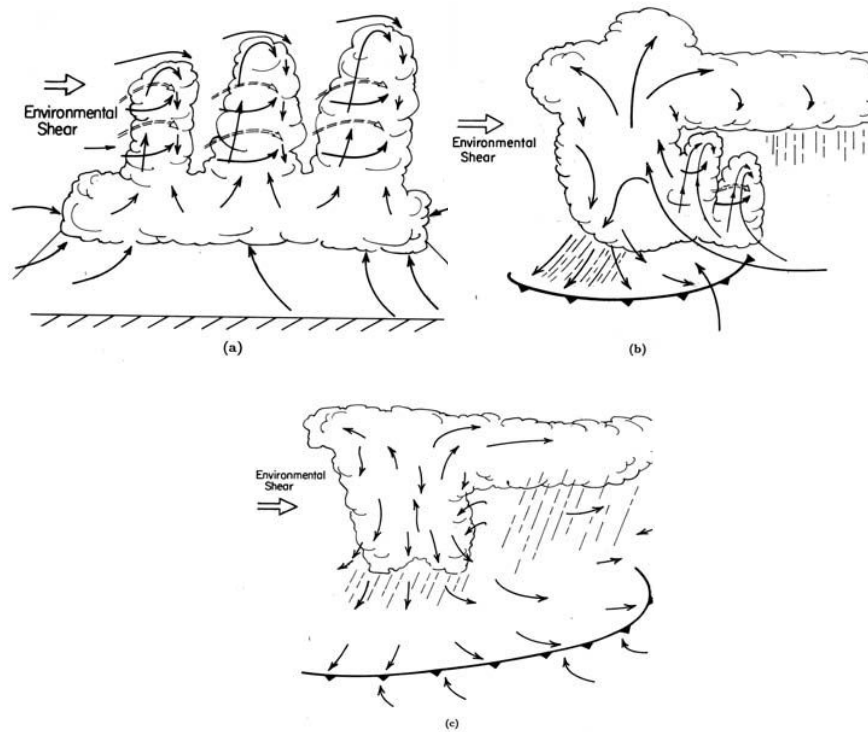


Figure 2-4. Schematic model of the lifecycle of an ordinary thunderstorm. (a) The cumulus stage is characterized by one or more towers fed by low-level convergence of moist air. Air motions are primarily upward with some lateral and cloud top entrainment depicted. (b) The mature stage is characterized by updrafts, downdrafts and rainfall. Evaporative cooling at low-levels forms a cold pool and gust front, which advances, lifting warm-moist, unstable air. An anvil at upper levels begins to form. (c) The dissipating stage is characterized by downdrafts and diminishing convective rainfall. Stratiform rainfall from the anvil cloud is also common. The gust front advances ahead of the storm preventing air from being lifted at the gust front into the convective storm. (From Cotton, [1990]).

2.1.2 Liquid Phase Clouds

2.1.2.1 Cloud Droplet Formation

The supersaturations required to nucleate drops by the chance collisions of water vapor molecules (i.e., *homogeneous nucleation*) greatly exceed the observed supersaturations in the atmosphere. Consequently, droplets do not form in natural clouds by homogeneous nucleation. Instead, they form by *heterogeneous nucleation* onto atmospheric aerosol.

Köhler [1926] first determined the equilibrium vapor pressure above small solution droplets (Figure 2-5). It can be seen from the curves shown in Figure 2-5 that below a certain droplet size, the relative humidity of the air adjacent to a solution droplet is less

than that which is in equilibrium with a plane surface of pure water at the same temperature (i.e., 100%). As a droplet increases in size, the lowering of the equilibrium vapor pressure above its surface due to the dissolved material becomes increasingly less and the equilibrium vapor pressure over a small curved droplet (Kelvin curvature effect) becomes the dominant influence.

Suppose a particle of NaCl with mass 10^{-19} kg is placed in air with a water supersaturation of 0.4% (indicated by the dashed line in Figure 2-5). As can be seen from Figure 2-5, the solution droplet will experience a supersaturation, and the droplet would grow by condensation. As it does so, the supersaturation adjacent to the surface of this solution droplet will initially increase, but even at the peak in its Köhler curve the supersaturation adjacent to the droplet is less than the ambient supersaturation. Consequently, the droplet will grow over the peak in its Köhler curve and down the right-hand side of this curve to form a fog or cloud droplet. A droplet that has passed over the peak in its Köhler curve and continues to grow is said to be *activated*.

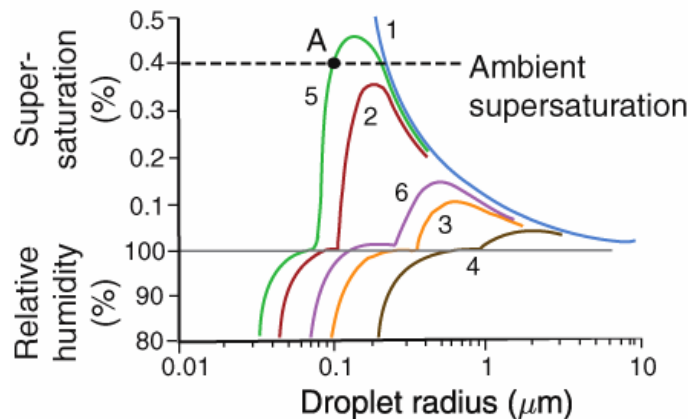


Figure 2-5. Variations of the relative humidity and supersaturation adjacent to droplets of (1) pure water (blue), and adjacent to solution droplets containing the following fixed masses of salt: (2) 10^{-19} kg of NaCl (red), (3) 10^{-18} kg of NaCl (orange), (4) 10^{-17} kg of NaCl (brown), (5) 10^{-19} kg of $(\text{NH}_4)_2\text{SO}_4$ (green), and (6) 10^{-18} kg of $(\text{NH}_4)_2\text{SO}_4$ (violet). Note the discontinuity in the ordinate at 100% relative humidity. Adapted from Rasool [1973].

Now consider a particle of $(\text{NH}_4)_2\text{SO}_4$ with mass 10^{-19} kg that is placed in the same ambient supersaturation of 0.4%. In this case, condensation will occur on the particle and it will grow as a solution droplet. At point A the supersaturation adjacent to the droplet is equal to the ambient supersaturation. If the droplet at A should grow slightly, the supersaturation adjacent to it would increase above the ambient supersaturation, and therefore the droplet would evaporate back to point A. If the droplet at A should evaporate slightly, the supersaturation adjacent to it would decrease below the ambient supersaturation, and the droplet would grow by condensation back to A in Figure 2-5. Hence, in this case, the solution droplet at A is in stable equilibrium with the ambient supersaturation. If the ambient supersaturation were to change a little, the location of A in Figure 2-5 would shift and the equilibrium size of the droplet would change accordingly. Droplets in this state are said to be *unactivated* or *haze droplets*. Haze droplets in the atmosphere can considerably reduce visibility by scattering light.

A sub-set of the atmospheric aerosol discussed in Chapter 3 serves as particles upon which water vapor condenses to form droplets that are activated and grow by condensation to form cloud droplets at the supersaturations achieved in clouds (~ 0.1 – 1%). These particles are called *cloud condensation nuclei* (CCN). It follows from the above discussion that the larger the size of a particle with a given chemical composition, the more readily it is wetted by water, and the greater its solubility, the lower will be the supersaturation at which the particle can serve as a CCN. For example, to serve as a CCN at 1% supersaturation, completely wettable but water insoluble particles need to be at least ~ 0.1 μm in radius, whereas soluble particles can serve as CCN at 1% supersaturation even if they are as small as ~ 0.01 μm in radius. Most CCN consist of a mixture of soluble and insoluble inorganic and organic components (called *internally-mixed nuclei*). The solubility of a particle has an important effect on its effectiveness as a CCN. For example, the initial minimum dry radius of a particle that is activated by a supersaturation of 0.1% is 0.075 μm if the particle is completely soluble. However, if the ratio of the soluble mass to the total mass of the particle is only 0.2, the particle would need to have a dry radius of 0.13 μm to be activated by a supersaturation of 0.1%.

Another aspect of CCN activity that is often overlooked is the wettability of the aerosol particle (i.e., the ability of water to spread out over the surface of the particle) as measured

by the contact angle of water on the particle. It is generally assumed that particles are completely wettable. However, this is by no means always the case [e.g., *Knight*, 1971]. For example, in the atmosphere there are a number of organic materials that are not wettable. To the extent that a substance has a non-zero contact angle, its ability to serve as a CCN will be hindered.

The surface tension of the solution formed by condensation onto a soluble particle will also affect the subsequent growth of the solution droplet. This is because for the Kelvin effect the energy barrier that has to be overcome for a droplet to be activated varies as the third power of the surface tension [*Wallace and Hobbs*, 2006]. The chemical components, concentrations, solubilities, and surface tensions of solution droplets that form in various environments are not well documented, and the effects of these parameters on droplet activation, individually and in combination are not well understood, but it is generally believed that surface tension effects are small.

Another factor of importance during droplet nucleation and vapor deposition growth is the diffusivity of vapor molecules near the surface of small droplets. Ordinarily diffusivities of water vapor that can be found in chemical handbooks do not take into account the kinetic effects of vapor diffusion when vapor molecules are within the mean free path distance of the droplet surface. To account for kinetic effects, the vapor diffusivities are modified with a so-called accommodation coefficient. There is strong disagreement in the literature regarding the value of the accommodation coefficient for atmospherically relevant conditions [*Shaw and Lamb*, 1999; *Laaksonen et al.*, 2005]. For example, the existence of film forming compounds in the aerosol may significantly reduce the mass accommodation. This parameter has a very strong effect on the number of droplets activated, with the latter tending to decrease with increasing values of this coefficient. Its effect is much stronger than many effects associated with changes in aerosol composition mentioned above [e.g., *Kreidenweis et al.*, 2003].

2.1.2.2 *Cloud Condensation Nuclei*

Because of the uncertainties in predicting the CCN nucleating ability of atmospheric particles, an empirical approach is generally taken by measuring the concentration of particles that serve as CCN at various prescribed supersaturations; this is called the *CCN*

supersaturation spectrum. The concentrations of CCN active at various supersaturations can be measured with a thermal gradient diffusion chamber, or other devices based on similar principles. A diffusion chamber may take a variety of geometric configurations, with the essential feature being that particles are statically or dynamically (with continuous flow) exposed to a steady supersaturation field created either by wetted plates held at different temperatures or by a streamwise gradient of temperature. By varying the temperature difference between the plates, it is possible to produce maximum supersaturations in the chamber that range from a few tenths of 1% to a few percent, which are similar to the inferred supersaturations that activate droplets in clouds [Wieland, 1956]. Worldwide measurements of CCN concentrations have not revealed any systematic latitudinal or seasonal variations. At a given location, CCN vary by several orders of magnitude with time, depending on the proximity of sources, wind direction, air mass type, precipitation and cloudiness [e.g., Twomey, 1960; Jiusto, 1966; Radke and Hobbs, 1969]. Near the earth's surface continental air masses generally contain larger concentrations of CCN than clean marine air masses (Figure 2-6). For example, the concentration of CCN in the continental air mass over the Azores, depicted in Figure 2-6, is about $\sim 300 \text{ cm}^{-3}$ at 1% supersaturation, while in the marine air mass over Florida it is $\sim 100 \text{ cm}^{-3}$, and in clean Arctic air it is only $\sim 30 \text{ cm}^{-3}$. The ratio of CCN (at 1% supersaturation) to the total number of particles in the air (CN) is $\sim 0.2\text{--}0.6$ in marine air; in continental air this ratio is generally less than ~ 0.01 but can rise to ~ 0.1 . The very low ratio of CCN to CN in continental air is attributable to the large number of very small particles, which are not activated at low supersaturations. Concentrations of CCN over land decline by about a factor of five between the planetary boundary layer and the free troposphere [Squires and Twomey, 1966; Hoppel et al., 1973; Hobbs et al., 1985]. Over the same height interval, concentrations of CCN over the ocean remain fairly constant, or may even increase with height reaching a maximum concentration just above the mean cloud height [Hoppel et al., 1973; Hudson, 1983; Hegg et al., 1990]. Ground-based measurements indicate that there is a diurnal variation in CCN concentrations at some locations, with a minimum at about 6 a.m. and a maximum at about 6 p.m. [Twomey and Davidson, 1970, 1972].

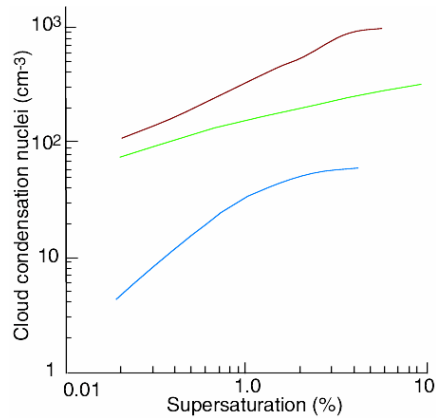


Figure 2-6. *Cloud condensation nucleus spectra in the boundary layer from measurements near the Azores in a polluted continental air mass (brown line), in Florida in a marine air mass (green line), and in clean air in the Arctic (blue line). From Wallace and Hobbs [2006] and data from Hudson and Yum [2002].*

The observations described above provide clues as to the origins of natural CCN. First of all it appears that the land acts as a major source of CCN, because the concentrations of CCN are generally high over land and decrease with altitude. Some of the soil particles and dusts that enter the atmosphere probably serve as CCN, but they do not appear to be a dominant source. The rate of production of CCN (active at a supersaturation of 0.5%) from burning vegetable matter is on the order of 10^{12} - 10^{15} per kg of material consumed [Eagan *et al.*, 1974b]. Thus, forest fires are a prolific source of CCN [Twomey, 1960; Twomey and Warner, 1967; Warner and Twomey, 1967; Warner, 1968, Hobbs and Radke, 1969; Woodcock and Jones, 1970; Stith *et al.*, 1981]. Although sea-salt particles enter the air over the oceans, they do not appear to be a dominant source of CCN, even over the oceans [Twomey, 1968, 1971; Radke and Hobbs, 1969; Dinger *et al.*, 1970; Hobbs, 1971], although, because of their solubilities and large sizes, they may enhance precipitation by serving as giant CCN.

There appears to be a widespread and probably a fairly uniform source of CCN over both oceans and land, the nature of which has not been definitely established. A likely candidate is gas-to-particle conversion, which can produce particles up to a few tenths of a micrometer in diameter that can act as CCN if they are soluble and wettable. Gas-to-particle conversion mechanisms that require solar radiation might be responsible for the

observed peak in CCN concentrations at ~6 p.m. Most CCN consist predominately of sulfates, although some organic material is usually present. Over the oceans, organic sulfur from the ocean (in the form of the gases dimethylsulfide (DMS) and methane sulfonic acid (MSA)) provides a source of CCN, with the DMS and MSA being converted to sulfate in the atmosphere [Charlson *et al.*, 1987; Hoppel, 1987; Luria *et al.*, 1989; Gras, 1990; Hegg *et al.*, 1991a,b; Ayers and Gras, 1991; Ayers *et al.*, 1991; Pandis *et al.*, 1994]. Evaporating clouds also release sulfate particles that are somewhat larger than non-cloud processed aerosol because of the additional material deposited onto them in clouds [Radke and Hobbs, 1969; Easter and Hobbs, 1974; Hegg *et al.*, 1980; Hegg and Hobbs, 1981; Hoppel *et al.*, 1986; Birmili *et al.*, 1999; Feingold and Kriedenweis, 2002]. It has been estimated that ~80% of sulfate mass globally is formed in the aqueous phase, and the remainder from the gas phase. As expected from the Köhler curves, larger sulfate particles serve more efficiently as CCN [Hegg, 1985; Leaitch *et al.*, 1986; Lelieveld *et al.*, 1997]. The production of sulfates (and maybe other soluble materials), followed by the release of these particles when the droplets evaporate, is an important mechanism for increasing the efficiency of CCN [Twomey and Wocjichowski, 1969; Hobbs, 1971; Easter and Hobbs, 1974]. There are also a number of anthropogenic sources of CCN, which are discussed in Chapters 3, 4 and 6.

2.1.2.3 *Effects of CCN on the Microphysical Structures of Clouds*

In a cloud, we are concerned with the growth of a large number of droplets in a rising parcel of air. As the parcel rises it expands, cools, and eventually reaches saturation with respect to liquid water. Further uplift and adiabatic cooling produces supersaturations that initially increase in proportion to the updraft velocity. CCN are activated as the supersaturation rises starting with the most efficient CCN. When the rate at which water vapor in excess of saturation, is equal to the rate at which water vapor condenses onto the CCN and droplets, the supersaturation in the cloud reaches a maximum value. The concentration of cloud droplets is determined at this stage (which generally occurs less than 100 m above cloud base) and is equal to the concentration of CCN activated by the peak supersaturation that has been attained. Subsequently, the growing droplets consume water vapor faster than it is made available by the cooling of the air, so the supersaturation begins to decrease. The haze droplets then begin to evaporate while the activated droplets continue to grow by condensation. The rate of growth of a droplet by condensation is inversely

proportional to its radius, therefore the radius of the smaller activated droplets grow faster than that of the larger droplets. Consequently, in this simplified model, the size distributions of the droplets in the cloud become increasingly narrower with time (that is, the droplets approach a *monodispersed* distribution). This sequence of events is illustrated by the results of theoretical calculations shown in Figure 2-7.

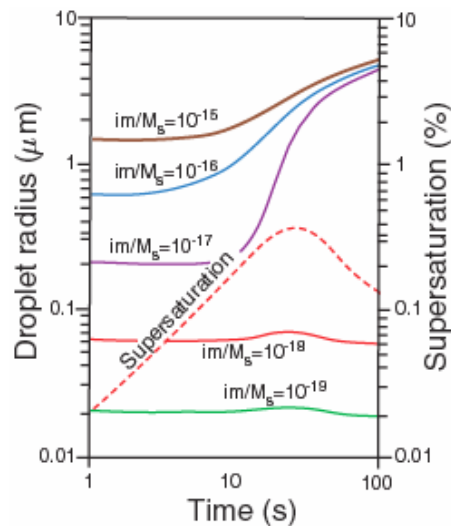


Figure 2-7. Theoretical computations of the growth of cloud condensation nuclei by condensation in a parcel of air rising with a speed of 60 cm s^{-1} . A total of 500 CCN cm^{-1} was assumed with im/M_s values as indicated; m the mass of material dissolved in the droplet, M_s the molecular weight of the material, and i its van't Hoff factor (i.e., the number of ions produced by each molecule of the material when it dissolves). Thus, im/M_s is the effective number of kilomoles of the material in the dissolved droplet. One can think of the terms im as representing the particular chemical properties of the salt. Note how the droplets that have been activated (brown, blue and purple curves) approach a monodispersed size distribution after just 100 s. (i.e. $\sim 60 \text{ m}$ above cloud base). The variation with time of the supersaturation of the air parcel is also shown (dashed red line). From Wallace and Hobbs [2006], based on data from Howell [1949].

Comparisons of cloud droplet size distributions measured a few hundred meters above the bases of non-precipitating warm cumulus clouds with droplet size distributions computed assuming growth by condensation for about 5 min show good agreement. The droplets produced by condensation during this time period extend only up to about $10 \mu\text{m}$ in radius. Moreover, as mentioned above, the rate of increase in the radius of a droplet growing by condensation is inversely proportional to the drop radius, therefore, the rate of growth decreases with time. It is clear, therefore, as first noted by Reynolds [1877], that growth by condensation alone in warm clouds is much too slow to produce raindrops with radii of

several millimeters. Yet rain does form in clouds that contain only water drops. The enormous increases in size required to transform cloud droplets into raindrops is illustrated by the scaled diagram shown in Figure 2-8. For a cloud droplet 10 μm in radius to grow to a raindrop 1 mm in radius requires an increase in volume of one millionfold! However, only about one droplet in a million (about 1 liter⁻¹) in a cloud has to grow by this amount for the cloud to rain. The mechanism responsible for the selective growth of a few droplets into raindrops in warm clouds is discussed in Section 2.2.1.

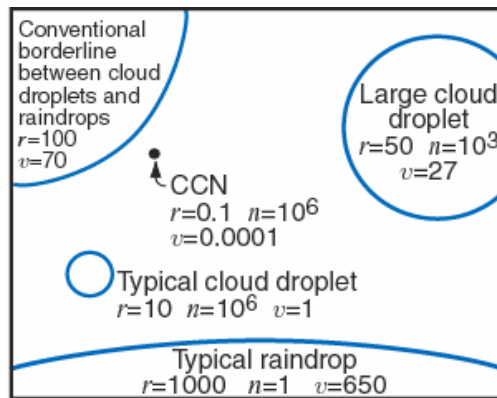


Figure 2-8. Relative sizes of cloud droplets and raindrops; r is the radius in micrometers, n the number per liter of air, and v the terminal fall speed in centimeters per second. The circumference of the circles are drawn approximately to scale, but the black dot representing a typical CCN is twenty-five times larger than it should be relative to the other circles. From Wallace and Hobbs [2006].

Since the concentration of CCN generally increases in passing from oceanic air sheds to continental air sheds to urban environments, the concentrations of cloud droplets likewise increase, and the droplet growth rate with altitude above cloud base decreases, at least for non-precipitating clouds [e.g., Gerber, 1996]. For example, droplet concentrations in non-polluted, non-precipitating marine cumulus clouds are generally less than 100 cm^{-3} while they can reach values over 1000 cm^{-3} in a polluted environment [Squires, 1958], see Figure 2-9. As we will see in Section 2.2.1, clouds with large concentrations of droplets are more colloidally stable and less likely to precipitate than clouds with small concentrations of droplets.

The effects of CCN from anthropogenic sources on cloud structures and precipitation are discussed in Chapter 5 and 6.

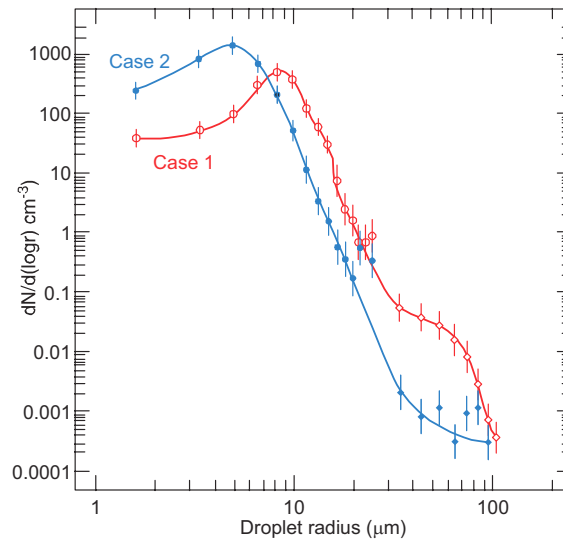


Figure 2-9. Cloud droplet number distributions measured in stratocumulus clouds in the vicinity of the Azores by the FSSP-100 (circles) and PMS 1D (diamonds) cloud probes, averaged over 15 km of flight path for case 1—clean marine air (red symbols and curve), and averaged over 4 km of flight path for case 2—continentally influenced air (blue symbols and curve). The vertical bars are the geometric standard deviations of the droplet concentrations. From Garrett and Hobbs [1995].

2.1.3 Ice Phase Processes

2.1.3.1 Nucleation of Ice

Ice particles can form either homogeneously or heterogeneously on some form of ice nuclei (IN). Homogeneous nucleation can take place either directly from the vapor or by freezing of cloud droplets. However, homogeneous nucleation of ice crystals from the vapor, or the chance formation of an embryo of ice-like structure of critical size, requires very high supersaturations with respect to ice and such low temperatures that it does not take place in the troposphere. On the other hand, homogeneous freezing of supercooled droplets by the chance formation of a cluster of ice-like embryos can occur in the atmosphere.

For homogeneous freezing to occur, enough ice-like water molecules must come together within the droplet to form an embryo of ice large enough to survive and grow. If an ice embryo within a droplet exceeds a certain critical size, its growth will produce a decrease in the energy of the system. On the other hand, any increase in the size of an ice embryo smaller than the critical size causes an increase in total energy. In the latter case, from an energetic point of view, the embryo is likely to break up.

Since the numbers and sizes of the ice embryos that form by chance aggregations increase with decreasing temperature, below a certain temperature (which depends on the volume of water considered) freezing by homogeneous nucleation becomes a virtual certainty. Homogeneous nucleation occurs in about one second at about -41°C for droplets about $1\ \mu\text{m}$ in diameter, and at about -35°C for drops $100\ \mu\text{m}$ in diameter. An analogous freezing process occurs for unactivated droplets or haze particles at temperatures below -40°C , a process for ice formation in cirrus clouds (*DeMott*, 2002). Hence, in the atmosphere, homogeneous nucleation by freezing generally occurs only in high clouds or high latitudes.

If a droplet contains a rather special type of particle, called a *freezing nucleus*, it may freeze by a process known as *heterogeneous nucleation* in which water molecules in the droplet collect onto the surface of the particle to form an ice-like structure that may increase in size and cause the droplet to freeze. Since the formation of the ice structure is aided by the freezing nucleus, and the ice embryo also starts off with the dimensions of the freezing nucleus, heterogeneous nucleation can occur at much higher temperatures than homogeneous nucleation.

If the particle that initiates freezing is contained within the droplet, it is called an immersion freezing nucleus. However, cloud droplets may also be frozen if a suitable particle in the air comes into contact with the droplet, in which case freezing is said to occur by *contact freezing*, and the particle is referred to as a *contact nucleus*. Laboratory experiments suggest that some particles can cause a drop to freeze by contact freezing at temperatures several degrees higher than if they were embedded in the drop [*Fletcher*, 1962; *Levkov*, 1971; *Gokhale and Spengler*, 1972; *Pitter and Pruppacher*, 1973].

Recent laboratory experiments by *Durant and Shaw* [2005] showed that as droplets evaporate, embedded aerosol particles become increasingly likely to penetrate the air-water interface layer and promote freezing. They interpreted this as evidence that contact freezing may be just as effective from the inside-out as from the outside-in.

Certain *particles* in the air also serve as centers upon which ice can form directly from the vapor phase. These particles are referred to as *deposition nuclei*. Ice can form by deposition provided that the air is supersaturated with respect to ice and the temperature is low

enough. If the air is supersaturated with respect to water, a suitable particle may serve either as a *condensation-freezing* nucleus (in which case liquid water first condenses onto the particle and subsequently freezes) or as a *deposition nucleus* (in which case there is no intermediate liquid phase, at least on the macroscopic scale). It is generally thought that condensation-freezing is preferred at smaller supercoolings and large supersaturations, while deposition is preferred at large supercoolings and small supersaturation. In practice, it is not easy to distinguish between deposition and condensation-freezing modes.

2.1.3.2 Properties of Ice Nuclei

If we refer to an ice-nucleating particle in general, without specifying its mode of action, we call it an *ice nucleus* (IN). However, it should be kept in mind that the temperature at which a particle can cause ice to form depends, in general, upon the mechanism by which the particle nucleates the ice as well as upon the previous history of the particle. The basic distinction that has to be made is whether nucleation is from the vapor or from the liquid phase [Vali, 1985].

Particles with molecular spacings and crystallographic arrangements similar to those of ice (which has a hexagonal structure) tend to be effective as ice nuclei, although this is neither a necessary nor a sufficient condition for a good ice nucleus. Most effective ice nuclei are virtually insoluble in water. Some inorganic soil particles (mainly clays) can nucleate ice at fairly high temperatures (i.e., above -15°C), and they probably play an important role in nucleating ice in clouds. Desert dust is known to be very good ice nuclei [DeMott *et al.*, 2003a]. For example, in one study, 87% of the snow crystals collected on the ground had clay mineral particles at their centers and more than half of these were kaolinite [Kumai, 1951]. Of course, it is only circumstantial evidence that they served as ice nuclei. Many organic materials are effective ice nucleators [Schnell and Vali, 1976a]. Decayed plant leaves contain copious ice nuclei, some active as high as -4°C . Ice nuclei active at -4°C have also been found in seawater rich in plankton. In addition, some plant pathogenic bacteria have also been found to be effective ice nuclei at temperatures as high as -2°C [Vali *et al.*, 1976; Yankofsky *et al.*, 1981; Levin and Yankofsky, 1983; Levin *et al.*, 1987]. Recently Von Blohn *et al.* [2005] have identified pollen as good ice nuclei at warm temperatures.

In some cases, after a particle has served as an ice nucleus and all of the visible ice is then evaporated from it, but the particle is not warmed above -5°C or exposed to a relative humidity with respect to ice of less than 35%, it may subsequently serve as an ice nucleus at a temperature a few degrees higher than it did initially [Roberts and Hallett, 1968]. This is referred to as *preactivation*. Thus, for example, preactivated nuclei may be transferred between sequential wave clouds and act at a higher temperature for the second and later clouds. However, preactivation is lost if the initially activated ice nucleus is either heated above at least -5°C and/or is dehydrated to less than $\sim 35\%$ relative humidity with respect to ice. Because preactivation can be lost if the particles are warmed or dehydrated prior to testing in an IN counter, this behavior creates a significant dilemma for IN measurements in almost any sampling scenario.

2.1.3.3 Variations of ice nuclei and ice particle concentrations

Ice nucleus concentrations can sometimes vary by several orders of magnitude over several hours (see also Chapters 5 and 6). Historically, ice nuclei concentrations have been assumed as predictors of ice particle concentrations. Laboratory studies in the 1940's and 1950's using systems for low temperature processing of ice nuclei collected on filters indicated that the variability in ice nuclei concentration was strongly a function of temperature. Fletcher [1962] derived an empirical relationship relating the increase of concentration of ice nuclei with decreasing temperature:

$$\ln N = a(T_1 - T) \quad (2.1)$$

where N is the concentration of active ice nuclei per liter of air, T is the air temperature, and T_1 is the temperature at which one ice nucleus per liter is active (typically about -20°C) and a varies from about 0.3 to 0.8. For $a = 0.6$, eqn. (2.1) predicts that the concentration of ice nuclei increases by about a factor of 10 for every 4°C decrease in temperature. In urban air, the total concentration of aerosol is on the order of 10^8 liter^{-1} and only about one particle in 10^8 acts as an ice nucleus at -20°C .

Later laboratory studies [e.g. Huffman and Vali, 1973; Huffman, 1973a,b] could not reproduce Fletcher's N - T empirical relationship. Measurements in a variety of field campaigns using a continuous flow diffusion chamber exhibited considerable variability in IN concentration [DeMott et al., 2003a; Rogers et al., 1998; Rogers et al., 2001; Prenni et al., 2007]. The variability in ice nuclei concentration is likely not a simple function of

temperature but also depends on thermodynamical, dynamical and aerosol characteristics [DeMott *et al.*, 1994].

The activity of a particle as a condensation-freezing or a deposition nucleus depends not only on the temperature but also on the supersaturation of the ambient air. The effect of supersaturation on measurements of ice nucleus concentrations is shown in Figure 2-10, where it can be seen that at a constant temperature the greater the supersaturation with respect to ice the more particles serve as ice nuclei. The empirical equation to the best-fit line to these measurements (the red line in Figure 2-10) is

$$N = \exp\left\{a + b[100(S_i - 1)]\right\} \quad (2.2)$$

where N is the concentration of ice nuclei per liter, and S_i is the supersaturation with respect to ice, $a = -0.639$ and $b = 0.1296$ [Meyers *et al.*, 1992]. These measurements were obtained using a continuous flow diffusion chamber (CFDC), which limited data suggests exhibits roughly a factor of ten higher concentrations of IN at warmer temperatures than older devices such as the filter-processing systems. Recognizing the need to allow vertical and horizontal variations in IN concentrations in mesoscale model simulations, Cotton *et al.* [2003] modified equation (2.2) to include the prognostic variable N_{IN} :

$$N_i = N_{IN} \exp [12.96 (S_i - 1)], \quad (2.3)$$

where $T < -5^\circ\text{C}$. The variable N_{IN} can be deduced from continuous flow diffusion chamber data and used as a forecast variable in regional simulations [i.e. van den Heever *et al.*, 2006; van den Heever and Cotton, 2007]. Equations (2.1), (2.2) and (2.3) only represent initial ice particle formation on IN and do not necessarily represent actual ice particle concentrations because other processes such as ice multiplication (see Section 2.1.3.4), sedimentation, breakup, and advection can greatly influence the concentrations of ice particles. Note that equation (2.3) allows for both horizontal and vertical variations in IN. Because the aerosol contributing to IN are large and large aerosol generally decrease with height [Georgii and Kleinjung, 1968; DeMott *et al.*, 2003b], we expect that IN concentrations generally decrease with height as well.

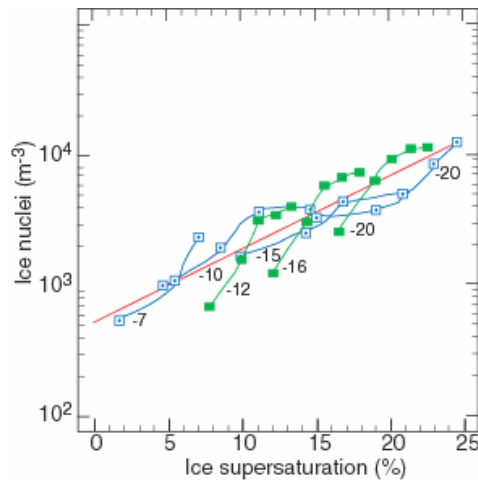


Figure 2-10. *Ice nucleus concentration measurements versus ice supersaturation; temperatures are noted alongside each line. All data were obtained at ground level. The red line is eqn. (4.2). Blue squares are data from Rogers [1993]; green squares are from Al-Naimi and Saunders [1985]. From Wallace and Hobbs [2006]’s adaptation of the Meyers et al.[1992] figure.*

One should not therefore be surprised that many observations of ice particle concentrations do not show a good correlation with temperature [Gultepe et al., 2001; Field et al., 2005]. Gultepe et al. [2001], for example, compiled data from the glaciated regions of stratus clouds for a number of field campaigns and found that ice crystals smaller than 1000 μm diameter do not show a good correlation with temperature and that the concentrations of these smaller ice particles varied up to three orders of magnitude, for a given temperature (see Figure 2-11). On the other hand, measurements of ice particle concentrations in wave clouds where only “initial” ice particles are likely [Cooper and Vali, 1981], showed ice particle concentrations increasing with decreasing temperature.

In summary, we see that there remain many unanswered questions regarding the concentrations of ice nuclei, their composition, their activation relative to different environmental factors, and their relationship to ice crystal concentrations. Work has been hampered by severe difficulties in precise measurement of IN (see Chapters 5 and 6). Moreover, current field deployable devices for measuring IN do not take into account activation of IN by contact freezing. Fletcher’s or Meyers empirical curves are still used and often misused in numerical models, ranging from cloud-resolving models to GCMs. These curves at best only represent the concentrations of ice particles initially formed in clouds and probably rarely represent ice particle concentrations in most cloud systems.

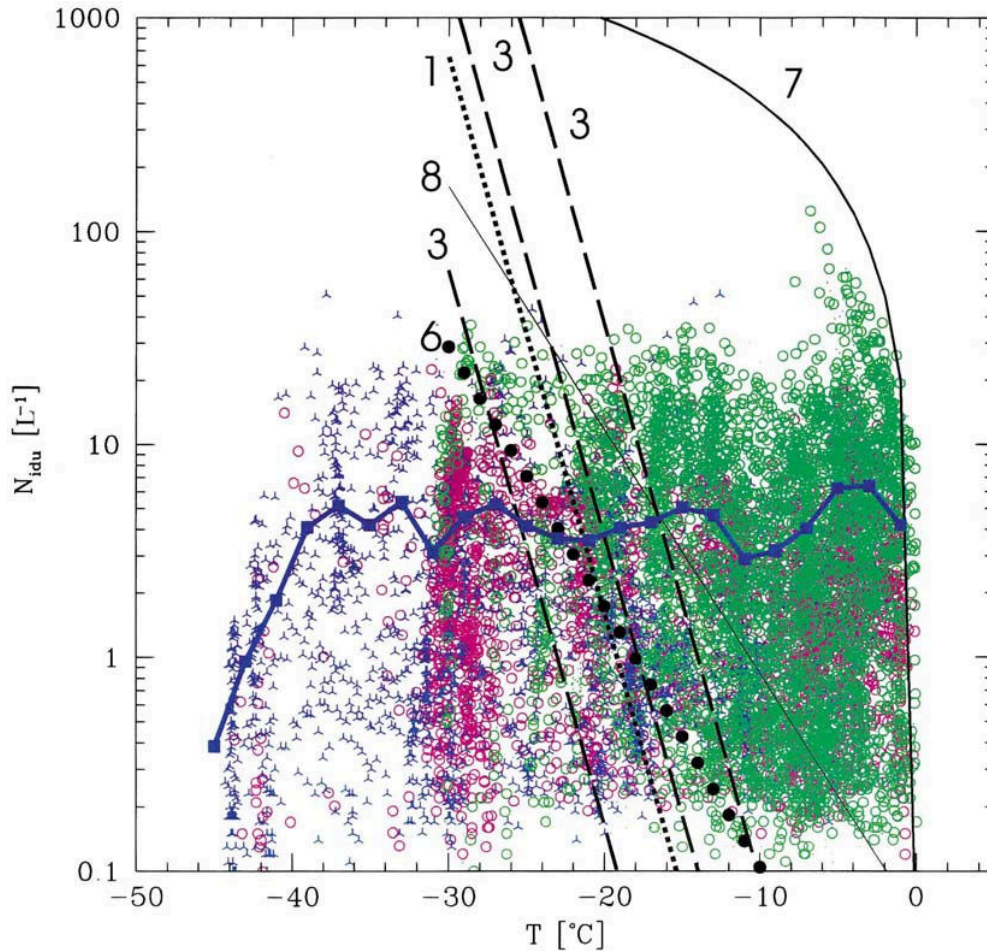


Figure 2-11. Concentrations of ice particles, greater than $125 \mu\text{m}$, from 2D-C probe measurements versus T at standard conditions during BASE (open green circles), FIRE.ACE (blue triples) and CFDE (open red circles) and from the earlier studies (black lines). Ice particles concentrations averaged over 2°C intervals for all projects is shown with a blue line. The thick solid line (7) is for Young [1974], dots (1) for Fletcher [1962], dashed lines (3) for Huffman and Vali [1973] filled circles (6) for a fit applied to Rogers et al. [1996] observations and the thin solid line (8) for Meyers et al. [1992]. From Gultepe et al. [2001]. Copyright © 2001 Royal Meteorological Society.

2.1.3.4 Concentrations of Ice Particles in Clouds: Ice Multiplication

As we have seen, it has become increasingly evident that concentrations of ice crystals in "real" clouds are not always represented by the concentrations of IN measured or expected to be activated in such environments. In particular, it has been found that at temperatures warmer than -10°C , the concentration of ice crystals can exceed the concentration of IN activated at cloud top temperature by as much as three or four orders of magnitude [Braham, 1964; Koenig, 1963; Mossop, 1970; Mossop and Ono, 1969; Mossop et al., 1967,

1968, 1972; *Magono and Lee*, 1973; *Auer et al.*, 1969; *Hobbs*, 1969; *Hobbs*, 1974]. The effect is greatest in clouds with broad drop-size distributions [*Koenig*, 1963; *Mossop et al.*, 1968, 1972; *Hobbs*, 1974].

Some explanations or hypotheses that have been proposed to account for the high ice particle concentrations observed in some clouds are as follows:

- Ice multiplication by fracturing of fragile ice crystals, which may breakup during collision with each other. [*Vardiman*, 1978].
- Fragmentation of large drops during freezing. [*Mason and Maybank*, 1960].
- Secondary ice particle formation during ice particle riming. (*Hallett and Mossop*, 1974; *Mossop and Hallett*, 1974).
- Enhanced ice nucleation in the presence of spuriously high supersaturations. [*Hobbs and Rangno*, 1985].
- Secondary ice particle generation during evaporation of ice particles (*Oraltay and Hallett*, 1989; *Dong et al.*, 1994).

Of these processes, the one that has been given the most attention and quantified in models is secondary ice particle formation by the rime-splinter process. Laboratory studies by *Hallett and Mossop* (1974) and *Mossop and Hallett* (1974), confirmed by *Goldsmith et al.* (1976) have indicated that copious quantities of splinters are produced during ice particle riming under very selective conditions. These conditions are:

- Temperature in the range of -3 to -8C.
- A substantial concentration of large cloud droplets ($D > 24 \mu\text{m}$).
- Large droplets coexisting with small cloud droplets ($D < 12.3 \mu\text{m}$).

An optimum average splinter production rate of 1 secondary ice particle for 250 large droplet collisions occurred at a temperature of -5C.

This process is consistent with observations of the greatest departure from IN estimates of ice crystals when clouds contain graupel particles and frozen raindrops and is consistent with field observations (*Hobbs and Cooper* (1987).

There is much indirect or inferential evidence that evaporation enhances ice crystal concentrations. This evidence is perhaps more intriguing than it is compelling. Some field studies have related unusually high ice nuclei numbers or unusual increases in ice crystal numbers to circumstances in which clouds were evaporating. *Cooper* [1995], for example, found a 100-fold increase in ice crystal concentrations in the evaporation region of orographic layer clouds. The largest ice enhancements in the *Cooper* study were observed in clouds with temperatures approaching the onset temperature for homogeneous freezing. Smaller enhancements were found in warmer clouds and no enhancements were found warmer than about -20°C . Further evidence of the possible role of evaporation nucleation has been presented by *Field et al.* [2001] and *Cotton and Field* [2002]. They show observational evidence and supporting parcel modeling calculations from wave cloud studies that suggest ice had to form close to the downstream edge of wave cloud. Ice production coincident with the start of the liquid cloud, or earlier, would have suppressed the observed liquid cloud. Some of the observations of rapid ice crystal concentration enhancement versus expected IN concentrations in cumulus cloud studies of *Hobbs and Rangno* [1985; 1990] and *Rangno and Hobbs* [1994] were also observed to originate in close proximity to regions of cloud evaporation. *Stith et al.* [1994] followed the development of ice in a cumulus turret near its top at -18°C . During the updraft stages, low ice concentrations were observed in the turret (similar to what would be expected from primary ice nucleation), but during the downdraft stages, the ice concentrations increased by an order of magnitude. This observation cannot be explained by rime splintering.

In summary, it is unlikely that all primary and secondary ice-forming processes have been quantitatively identified. Other mechanisms may sometimes operate, but their exact nature remains a mystery. Moreover, our ability to measure small ice crystals, in particular, has significant errors and need improvement. Consequently, there are large uncertainties associated with our ability to simulate the affect of aerosols on the initiation of ice, and subsequent impacts on precipitation. This remains as one of the critical problems in cloud physics.

2.2 Formation of Precipitation

Precipitation-sized particles can form by two mechanisms, known as the *collision-coalescence* and the *ice particle* mechanisms. The collision-coalescence mechanism can operate in clouds containing droplets, whether they are situated above or below the 0°C level. The ice particle mechanism can operate only in clouds with temperatures below 0°C and containing some ice particles.

2.2.1 The Collision-Coalescence Mechanism

This mechanism for rainfall production involves the initial formation of a few cloud drops with radii of about 20 μm by condensation onto CCN, followed by their rapid and substantial growth as they fall through the air and collide with smaller cloud droplets. If a drop increases in radius from 20 μm to a radius typical of raindrops, say 2 mm, its volume increases by a factor of one million. In other words, about one million cloud droplets have to combine to form one raindrop!

Due to the flow of air around a falling drop, a drop will not collect all of the droplets that lie in its path. Calculated values of the *collision efficiency*, defined as the ratio of the cross-sectional area over which droplets are collected to the geometric cross-sectional area of the collector drop, are shown in Figure 2-12. This figure shows that the collision efficiency is negligible (<0.1) until a collector drop attains a radius of about 20 μm . Hence, the need for a few droplets to grow to 20 μm in radius by condensation if a cloud is to form raindrops by the collision-coalescence mechanism. As the droplet grows by condensation alone, the rate of increase in the radius slows (Figure 2-13). In contrast, after a droplet has reached a radius of 20 μm its collision efficiency increases rapidly with increasing size (Figure 2-13), so the droplet grows increasingly fast by collision. Moreover, as droplets get larger their cross sectional areas and fall velocities increase thereby increasing the collection kernel between large and small drops. Were it not for the fact that growth by collisions takes over as growth by condensation becomes negligible, many clouds would not rain.

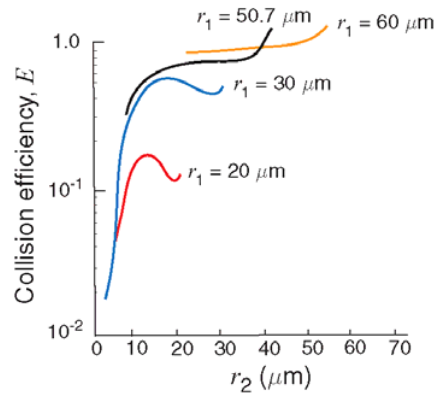


Figure 2-12. Calculated values of the collision efficiency, E , for collector drops of radius r_1 with droplets of radius r_2 . From Pruppacher and Klett [1997].

Another factor effecting droplet growth by collection is the efficiency with which colliding drops coalesce. There is a good database of the efficiencies of drop collision efficiencies [Beard and Ochs, 1993] but somewhat poorer knowledge of the coalescence efficiencies [Whelpdale and List, 1971; Levin et al., 1973; Beard and Ochs, 1993; Ochs et al., 1995], between drops over the range 1-300 microns. It is generally assumed that coalescence efficiencies are close to unity for small droplet collisions.

The basic problem is how do drops grow to a radius of 20 μm or greater fast enough to allow precipitation growth during the lifetime of clouds?

For an idealized cloud, the mean volume droplet radius at any height above cloud base, can be derived from the adiabatic water content at that height, $q_c(h)$, and the number concentration of activated nuclei N as

$$R_v = (q_c(h)/(4/3\pi\rho_w N))^{1/3} \quad (2.4)$$

For example, at a droplet concentration of 100 cm^{-3} , q_c must reach a value of 3.2 g m^{-3} (slightly less than 2 km of vertical ascent), for the mean volume radius to reach 20 μm . Since after CCN activation, the droplet spectrum approaches a monodispersed distribution, there are no droplets significantly bigger than R_v . The adiabatic assumption provides an estimate of the maximum droplet size, so that clouds growing in a polluted environment

($N > 500 \text{ cm}^{-3}$) should not be able to generate $20 \text{ }\mu\text{m}$ radius droplets during their lifetime, based on the simplistic adiabatic model alone.

Four mechanisms have been hypothesized to explain how larger droplets or precipitation embryos can form:

- Role of giant cloud condensation nuclei.
- Turbulence influences on condensation growth.
- Turbulence influence on droplet collision and coalescence.
- Radiative cooling of drops to form precipitation embryos.

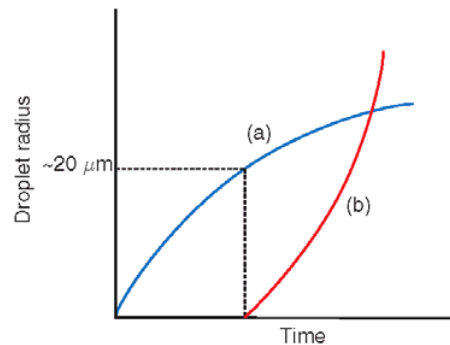


Figure 2-13. Schematic curves of the growth of a drop (a) by condensation (blue curve) and (b) by collection of droplets (red curve).

2.2.1.1 Role of Giant Cloud Condensation Nuclei (GCCN)

Observations reported by *Woodcock* [1953], *Nelson and Gokhale* [1968], *Hindman* [1975], *Johnson* [1976; 1982], and *Hobbs et al.* [1980] have shown the presence of potentially significant concentrations of aerosol particles of sizes as large as $100 \text{ }\mu\text{m}$. Their concentrations are $\sim 10^{-3} \text{ cm}^{-3}$ [*Woodcock*, 1953], that is, about one in 10^5 or 10^6 CCN are giant particles. Nevertheless, these particles can have a significant effect on the development of precipitation by serving as coalescence embryos [*Johnson*, 1982; *Feingold et al.*, 1999; *Yin et al.*, 2000a]. The droplet that forms is large enough for coalescence to start immediately even before the droplet reaches its critical size based on the Köhler

equation. This can occur if the nuclei are completely soluble (e.g., sea-salt particles) or are mixed particles with a soluble coating [e.g., mineral dust with a coating of sulfate, *Levin et al.*, 1996] or are very large and wettable. The presence of GCCN on precipitation formation has been investigated in a number of cloud resolving models, which show that their contribution to rain formation may be appreciable in polluted clouds but has little influence in clouds forming in clean airmasses [i.e. *Feingold et al.*, 1999; *Khain et al.*, 2000].

2.2.1.2 Turbulence influences on Condensation

While the adiabatic model assumes a uniform updraft and a constant droplet concentration, convective clouds are in fact made of a series of updrafts of diverse intensities. The least vigorous updraft at cloud base also produces the lowest droplet concentration during activation of the available CCN. Turbulence further contributes to entrainment of dry environmental air in clouds, hence reducing LWC below the adiabatic value and diluting the droplet concentration below its initial value after CCN activation. Convective cells with a significantly reduced concentration might generate bigger droplets than adiabatic cores, if they are further experiencing a convective ascent [*Baker et al.*, 1980; *Telford and Chai.*, 1980, and *Telford et al.*, 1984]. Turbulence however contributes also to the continuous mixing of the convective cells, hence smoothing out their differences in term of concentration and droplet growth.

Airborne measurements performed in cumulus clouds with the high resolution droplet spectrometer Fast-FSSP (see Chapter 6) reveal the occurrence of very narrow droplet spectra in cloud cores [*Brenguier and Chaumat*, 2001]. However, droplet spectra are often much broader than the narrow adiabatic reference, with droplet sizes extending from zero to the maximum predicted by the adiabatic model. This reflects the impact of mixing between convective cells that have experienced various levels of dilution with the entrained air. There are also airborne observations in stratocumulus clouds showing negative correlations between droplet concentration and droplet sizes [see for example Fig. 7 in *Pawlowska and Brenguier*, 2000]. This corroborates the hypothesis that fluctuations of the updraft intensity at cloud base or ascent of diluted cloud cells might contribute to the formation of droplets bigger than the adiabatic prediction based on the mean droplet concentration. In deeper clouds, airborne cloud traverses at a given level all look rather

similar in term of droplet concentration and sizes, suggesting that concentration/size correlations progressively dissipate due to continuous mixing.

Numerical simulations [Vaillancourt *et al.*, 2002; Shaw *et al.*, 1998] suggest that turbulence may also generate concentration fluctuations at the microscale by inertia in the regions of high vorticity, hence leading to superadiabatic droplet growth in the microcells with the lowest concentrations. This hypothesis was however contradicted by in situ measurements of the droplet spatial distribution at the microscale [Chaumat and Brenguier, 2001].

In summary, there is no observational evidence that turbulence contributes to the formation of precipitation embryos by enhanced condensation growth. In fact, stochastic processes induced by turbulence are not likely to enhance droplet growth because condensation is a cumulative process. To experience superadiabatic growth, droplets need to remain isolated in regions of higher supersaturation for a significant part of their ascent. The odds of this are low as mixing continuously redistributes droplets in the cloud. Turbulence is more likely to affect a discontinuous process like collision since once droplets coalesce, they cannot be separated.

2.2.1.3 Turbulence Influence on Droplet Collision and Coalescence

Turbulence can influence the collision and coalescence process in three ways:

- By enhancing collision efficiencies.
- By enhancing the collection kernels.
- By producing inhomogeneities in droplet concentration.

The collision efficiencies we discussed earlier were calculated in laminar or stagnant flow. In turbulent flow droplets will be accelerating and thereby be able to cross streamlines more efficiently than in laminar flow resulting in enhanced collision efficiencies. Large droplets, having more inertia will be affected more by turbulence than smaller drops. Calculations by Koziol and Leighton [1996] suggest that this effect is small for droplets smaller than 20 μ m diameter.

However, turbulence can also cause fluctuations on vertical fall speeds and horizontal motions, such that the collection kernel is enhanced [*Pinsky and Khain, 1997; Khain and Pinsky, 1997*], relative to that defined in laminar flow.

Because the collection rate is proportional to the square of droplet concentrations, inhomogeneities in droplet concentrations due to turbulence can produce enhanced regions of collection where the droplet concentrations are locally enhanced in, say regions of low vorticity [*Pinsky and Khain, 1997*]. This hypothesis has been examined in a cloud-resolving model by *Khain and Pokrovsky [2005]*.

2.2.1.4 Radiative cooling of drops to form precipitation embryos

Consider a population of droplets that resides near cloud top for a sufficiently long time. Those droplets will emit radiation to space quite effectively if the atmosphere above is relatively dry and cloud free. As a result, the droplets will be cooler than they would without considering radiative effects. This means that the saturation vapor pressure at the surface of the droplet will be lowered and the droplets will grow faster.

But radiation cooling is proportional to the cross sectional area of a droplet so that its effect is much greater on larger droplets than small ones [*Roach, 1976; Barkstrom, 1978; Guzzi and Rizzi, 1980; Austin et al., 1995*]. In fact, *Harrington et al. [2000]* have shown that in a marine stratocumulus environment, when droplets are competing for a limited supply of water vapor, the larger droplets grow so rapidly by radiative enhancement that droplets smaller than 10 μm in radius evaporate producing a bimodal size spectrum. This process is only effective in clouds where droplets reside near cloud top for time scales of 12 min or longer such as fogs, stratus, and stratocumulus. Cumulus clouds with vigorous overturning “expose” droplets to space for too short a time.

2.2.1.5 Mature phase of liquid phase precipitation formation

Once precipitation embryos form, they collect smaller droplets rapidly and they then transform into drizzle and raindrops in a matter of minutes if the liquid water content in clouds is great enough. The final size spectrum of the raindrops is determined by the liquid water content in the clouds as well as their trajectories through updrafts and downdrafts in the cloud. Moreover, raindrops may break up either spontaneously or by colliding with

other raindrops and breaking up. Thus, the final size-spectrum of raindrops is influenced by the breakup process as well.

In summary, the ultimate control on the initiation, evolution, and intensity of rainfall from warm clouds is the temporal-spatial structure of a cloud's updraft/downdraft and liquid water content (LWC). These properties along with the initial activated droplet population, provide the boundary conditions (i.e. time scales) for particle growth, that determine the intensity and duration of precipitation. That is, each droplet must first undergo nucleation, then condensation growth, followed by some mechanism of forming collection embryos, then stochastic collection, followed by continued raindrop collection of smaller drops and then breakup. All these steps take *time*. Thus critical to the formation of mature rain is whether or not the cloud lifetime and parcel lifetimes are long enough to allow all these steps to operate.

In simplest terms, clouds most likely to produce the most precipitation by exclusively liquid phase processes are maritime and warm-based. By maritime, we mean clouds forming in a clean atmosphere with low CCN concentrations. If a cloud is warm-based then its saturation mixing ratio at cloud base is high. For example, a cloud with a base temperature of 24C has a saturation mixing ratio of roughly 20g/kg, whereas one with a base temperature of 5C has a saturation mixing ratio of less than 6g/kg. Thus if a cloud with a warm base has a depth of, say, 3km it has a much greater potential of condensing a large amount of condensate than a cloud of similar depth having a higher, cold cloud base. We sometimes refer to warm-based, maritime clouds as being colloidally unstable [see *Cotton and Anthes*, 1989].

By contrast, a cloud, which is cold-based, and forms in a continental or an aerosol-polluted environment has a much smaller chance of producing precipitation and is said to be colloidally stable. The potential for liquid phase precipitation formation in most clouds will be between these two extremes.

2.2.2 Ice Particle Mechanisms

In regions of clouds lower than 0°C, supercooled water droplets can be present with or without coexisting ice particles. In Section 2.1.3, we discussed the nucleation of ice in

clouds and ice multiplication mechanisms. Here we are concerned with the growth of ice particles to precipitation sizes in mixed clouds.

As early as 1789 *Benjamin Franklin* [1789] wrote “It is possible that, in summer, much of what is rain, when it arrives at the surface of the Earth, might have been snow, when it began its descent, but being thawed, in passing through the warm air near the surface, it is changed from snow to rain.” This idea was not developed until the early twentieth century, when *Wegener* [1911] noted that ice particles would grow preferentially by vapor deposition in a mixed cloud. Subsequently, *Bergeron* [1933] and *Findeisen* [1938] developed this idea in a more quantitative manner.

In a mixed cloud dominated by supercooled droplets, the air is close to saturation with respect to liquid water and is therefore supersaturated with respect to ice. For example, air saturated with respect to liquid water at -10°C is supersaturated with respect to ice by 10%, and at -20°C , the air is supersaturated with respect to ice by 21%. These supersaturations with respect to ice are much greater than the supersaturations of cloudy air with respect to liquid water, which rarely exceed 1%. Consequently, in mixed clouds dominated by supercooled water droplets, ice particles will grow from the vapor phase much more rapidly than droplets. This can lead to a variety of ice crystal types, some of which may be large enough to precipitate. This process is generally referred to the “vapor growth stage” of ice particle growth.

In a mixed-phase cloud, ice particles can also grow by colliding with supercooled droplets, which then freeze onto them. This growth process, which is referred to as *riming*, can produce heavily rimed ice particles, graupel particles and, if the cloud is deep enough, contains sufficient supercooled water, and updrafts are strong, hailstones can form. Finally, ice particles in a cloud may collide and aggregate with each other, leading to larger particles, which are called *aggregates*. Unfortunately, the collision and coalescence efficiencies of ice particles riming cloud droplets are not well documented. Even more poorly quantified are the collision and coalescence efficiencies, and collection kernels among ice particles undergoing aggregation.

The growth of ice particles, first by deposition of water vapor followed by riming and/or aggregation, can produce precipitation-sized particles. If temperatures at ground level are

below 0°C, these particles will reach the ground as snow; if the surface temperature is above 0°C, the ice particles will partially melt, or melt completely, and reach the ground as wet snow or rain. An increase in the concentration of cloud droplets accompanied by decreases in the average size of the droplets (which can be caused by an increase in the concentration of CCN) may decrease growth by riming due to the lower collection efficiency of smaller droplets [Borys *et al.*, 2000, 2003].

In deep convective clouds, the rapidity of glaciation is dependent upon the presence of drizzle drops and large supercooled raindrops [Cotton, 1972; Koenig and Murray, 1976; Scott and Hobbs, 1977]. When CCN concentrations are high, liquid phase precipitation collection processes are suppressed and supercooled raindrops are few in number, small ice crystals must first grow to several hundred micrometers in diameter before they begin collecting cloud droplets. Then the riming process proceeds slowly until the ice particles have grown to millimeter-size. Furthermore, since riming is suppressed in clouds forming in air masses with high CCN concentrations, secondary ice particle production by the rime-splintering process [Hallett and Mossop, 1974; Mossop and Hallett, 1974] is suppressed as well.

If the updrafts and liquid water contents in deep cumulonimbi are large enough, graupel particles, frozen raindrops and large aggregates can serve as embryos for hailstone formation [Heymsfield *et al.*, 1980]. At first, the density of graupel particles is low as the collected frozen droplets are loosely compacted on the surface of the graupel particle. As the ice particle becomes larger, it falls faster, sweeps out a larger cross-sectional area, and its growth by collection of supercooled droplets increases proportionally. As the growth rate increases, the collected droplets may not freeze instantaneously upon impact, and thus flow over the surface of the hailstone filling in the gaps between collected droplets. The density of the ice particle, therefore, increases close to that of pure ice as the dense hailstone falls still faster, growing by collecting supercooled droplets as long as the cloud liquid water content is large. The ultimate size of the hailstone is determined by the amount of supercooled liquid water in the cloud and the time that the growing hailstone can remain in the high rainwater region. The time that a hailstone can remain in the high liquid water content region, in turn, is dependent on the updraft speed and the fall speed of the ice particle. If the updraft is strong, say 35-40 m/s, and the particle fall-speed through the air is only on the order of 1-2 m/s, then the ice particle will be rapidly transported into the anvil

of the cloud before it can take full advantage of the high liquid water content region. The ideal circumstance for hailstone growth is that the ice particle reaches a large enough size as it enters the high liquid water content region of the storm so that the ice particle fall speed nearly matches the updraft speed [Foote, 1984]. In such a case, the hailstone will only slowly ascend or descend while it collects cloud droplets at a very high rate. Eventually, the hailstone fall speed will exceed the updraft speed or it will move into a region of weak updraft or downdraft. The size of the hailstone reaching the surface will be greatest if the large airborne hailstone settles into a vigorous downdraft, as the time spent below the 0C level will be lessened and the hailstone will not melt very much. Thus, a particular combination of airflow and particle growth history is needed to produce large hailstones.

In summary, hail growth is most likely if the convective storm updrafts are strong, if the liquid water contents are large, the storm is deep and long-lived, and the melting level is low relative to the ground [Foote, 1984]. There is some limited modeling work that suggests the concentrations of CCN and IN are factors in hail formation [Danielsen, 1977].

2.2.3 Summary of Cloud Microphysical Processes

In preceding sections, we have seen that the evolution of precipitation in clouds can take on a variety of forms and involve numerous physical processes. The evolution of ice- phase precipitation processes is greatly dependent upon the prior or concurrent evolution of the liquid-phase. These processes, in turn, are dependent upon the characteristics of the air mass (i.e. aerosols), the liquid-water production of the cloud, the vertical motion of air within the cloud, the turbulent structure, and the time scales of the cloud. Illustrated in Figure 2-14 are the different precipitation paths that may occur depending upon whether the cloud is a cold-based continental cloud versus a warm-based maritime cloud. Remember from earlier discussions that we use the term maritime cloud to represent a very clean air mass and continental to represent one with much higher CCN concentrations. A polluted cloud would have still higher CCN concentrations. The figure does not note the speed by which these regimes can produce precipitation. We have pointed out earlier that a cloud with a vigorous warm rain process or what we refer to in the figure as a warm-based maritime cloud will produce precipitation much faster than a cold-based continental cloud.

The rapidity of glaciation of a warm-based maritime cloud is much faster than the cold-based maritime cloud since the presence of drizzle drops and supercooled raindrops once frozen can rapidly transform a cloud from an all water cloud to an ice-dominated cloud. This should not be interpreted to mean that the largest precipitation elements such as hail would occur in a warm-based maritime cloud. In fact, just the opposite can take place as a vigorous precipitation process lower in the cloud can deplete supercooled water amounts higher up and lower the trajectory of precipitation elements leading to smaller sized hailstones (see Chapter 8).

This diagram is used to illustrate two distinctly different regimes. In fact, there is a continuum of cloud types between these two extreme states. The heaviest precipitating clouds, and generally most efficient, are those that are warm-based and form in maritime airmasses. By contrast, clouds developing in a polluted airmass should be less efficient in producing precipitation than similar clouds with the same cloud base temperatures. This simple reasoning is valid only for single clouds and storms. As we will see in Chapter 7, in some cases a suppression or retardation of precipitation in a primary convective cell could lead to a transformation of a cloud into a long-lived squall line through the interaction of cold-pools with wind shear leading to self-propagating storm.

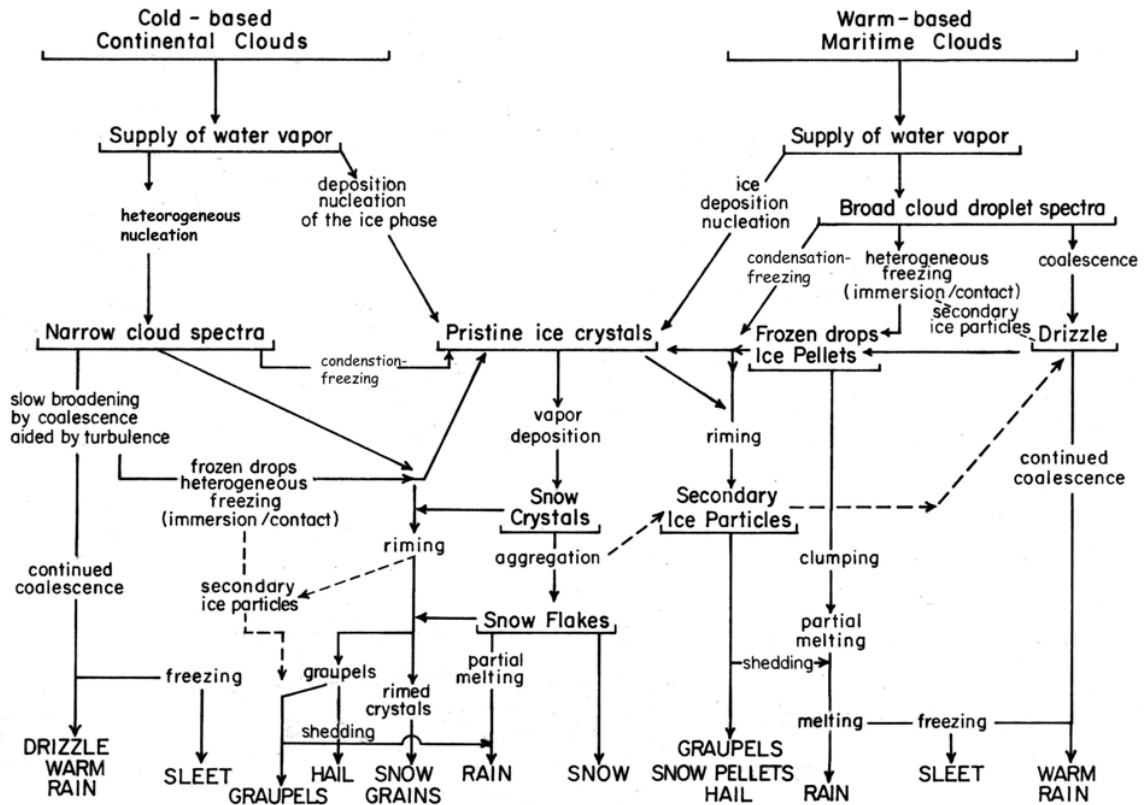


Figure 2.14. Flow diagram describing microphysical processes, including different paths for precipitation formation. (Adapted from Braham [1968]).

2.3 Precipitation Efficiency

The term *precipitation efficiency* has many definitions in the literature and generally refers to the fraction of either the water vapor input at cloud base or condensed water in cloud that falls out as precipitation. Instantaneous values of PE vary from near zero early in the lifetime of a cloud before precipitation has commenced to values exceeding 100% during the dissipation stages of a storm, when cloud-base moisture fluxes are near zero [Market *et al.*, 2003]. Doswell *et al.* [1996] suggest that PE is most meaningful when averaged over the storm lifetime. Market *et al.* [2003] propose that it is best to define a volume around a moving system and employ storm-relative winds in evaluating PE. In this way, storm-averaged PE can be obtained for a moving system. PE estimates from different studies are

problematic to compare because of differing definitions of PE, different data sources such as aircraft in situ versus radar measurements, and different time and spatial averaging [Hobbs *et al.*, 1980].

Fankhauser [1988] presented one of the most detailed studies of thunderstorm precipitation efficiency. Data were taken from seven storms during the Cooperative Convective Precipitation Experiment (CCOPE) using aircraft, rawinsondes, a surface mesonetwork and radar histories and calculated values ranging from 19% to 47%. Various environmental quantities, such as kinetic energy, cloud base area and height, and cloud base mixing ratio were found to be factors that had a strong positive correlation to PE levels. He found that variables such as the bulk Richardson number, the ratio of buoyant energy to the amount of wind shear, and convective available potential energy (CAPE), a measure of potential updraft strength, did not correlate well with PE.

Another strategy for estimating precipitation efficiencies is to use drying ratio (DR) as proposed by Smith *et al.* [2003].

$$\text{DR} = \text{total precipitation/vapor flux} \quad (2.5)$$

DR encapsulates the moisture budget of the large-scale air mass transformation. Because PE requires an estimate of vertical air velocity at cloud base, it is subject to rather large errors in those measurements. Since DR uses the ratio of precipitation to water vapor flux, it is easier to quantify than PE. Moreover, DR can be estimated using hydrogen and oxygen isotope analysis, which permits evaluation using streamflow or sapwood collected near a stream. Isotope analysis indicated a DR value of 43% for the combination of the coastal and Cascade mountain ranges in western Oregon and 48% for the southern Andes [Smith *et al.* 2005; Smith and Evans, 2006].

To date no one has made estimates of storm-averaged PE or DR for storms developing in environments containing different cloud-nucleating aerosol concentrations. Such work should be encouraged as a means of determining the impact of aerosols on precipitation while accounting for different water vapor and vertical air motion conditions.